

Atmospheric plasma sprayed coatings of nanostructured zirconia

Yi Zeng^{a,*}, S. W. Lee^a, L. Gao^b, C. X. Ding^b

^a*Sun Moon University, Department of Materials Engineering, Asan, South Korea*

^b*Shanghai Institute of Ceramics, Chinese Academy of Science, Shanghai, China*

Received 6 October 2000; received in revised form 10 April 2001; accepted 21 April 2001

Abstract

Nanostructured zirconia coating has been fabricated by atmospheric plasma spraying. The microstructure of the coating has been characterized with SEM and XRD, and the microhardness has been measured. The results show ZrO₂ coating possessed two kinds of structure. One was the poorly consolidated structure, which was composed of nanosized particles. The other was an overlapping structure, which consisted of micrometer size particles. The former was the main structure in the coating. The zirconia coating had the same phase composition as the starting powder and the thickness of coating was quite heterogeneous. The as-sprayed nano zirconia coating had a similar microhardness to sintered ZrO₂, which was much higher than the conventional counterpart. © 2001 Published by Elsevier Science Ltd. All rights reserved.

Keywords: Coatings; Microhardness; Microstructure; Plasma spraying; ZrO₂

1. Introduction

Nanoscale materials have received much attention in recent years due to their outstanding properties when compared to those of their micron-size counterparts.^{1–3} Various techniques have been used to prepare nanostructured materials, such as the sol-gel process,⁴ direct current reactive magnetron sputtering,⁵ radio frequency magnetron sputtering, etc.⁶ However, the process more likely to benefit from a short term, is deposition of coatings by a thermally activated process. Karthikeyan et al.⁷ developed a thermal spraying technique to produce nanoceramics powders and deposits. Tellkamp et al.⁸ sprayed nanocrystalline Inconel 718 powders, with a grain size range of 19–26 nm, by using a high velocity oxygen fuel (HVOF). The resulting coating remained nanocrystalline with a grain size range of 27–47 nm. Recently, nanocrystalline 316-stainless steel coatings were produced by using HVOF.⁹ Increases in microhardness values were observed in the as-sprayed nano coatings. Results from transmission electron microscopy analysis on the nano coatings showed that fractions of the nanocrystalline powders did not melt during the HVOF spraying.

In the present work, on the basis of successfully producing the nano titanium oxide coating by Dr. Zhu,¹⁰

nanostructural zirconia coatings were deposited by atmospheric-plasma spraying and characterized with scanning electron microscopy (SEM) and X-ray diffraction (XRD). Zirconia has a wide application in fields of thermal barrier materials and oxygen sensors, and an as-prepared nanostructured zirconia coating may have a potential application in these fields.

2. Experimental procedure

2.1. Preparation of the nano zirconia powder

The nano zirconia powders were fabricated by the chemical reaction method. The preparation process was as follows: put ZrOC₁₂ and Y(NO₃)₃ together in the water, then stir and add ammonia by dropping until the pH value is larger than 9. The precipitate was washed with water at least six times, and then washed with alcohol three times. After drying at 120°C for 24 h, the powder was milled. Lastly the powders were calcined at 600°C for 2 h.

2.2. Preparation of the nanostructured zirconia coating

The A-2000 atmospheric plasma spraying equipment (Sulzer Metco AG, Switzerland) was used to deposit nanostructured zirconia coating. The powders were fed

* Corresponding author. Fax: +82-418-543-2798.

E-mail address: zyidq_2000@yahoo.com (Y. Zeng).

by using the twin-hopper system. Table 1 summarizes the experimental conditions. The coatings were deposited on stainless steel substrates.

2.3. Structural analysis of the nanostructured zirconia coating

X-Ray diffraction analysis was performed on the starting powder and the as-sprayed coating of phase identification and determination of the grain size. A Siemens D5000 diffractometer operating with CuK_α ($\lambda = 1.54056 \text{ \AA}$) radiation was used. The integral breadth method was used to determine the grain size of the starting powder and the coating. The grain size was determined on the basis of the Scherrer equation using the two high intensity peaks located at low angles,¹¹

$$B(2\theta) = 0.9\lambda/D\cos\theta \quad (1)$$

Where D is the average dimensions of crystallites, B is the broadening of the diffraction line measured at half maximum intensity, λ is the wave length of the X-ray radiation and θ is the Bragg angle.

The surface and cross-section morphologies of the coating were determined with a JEOL JSM 6400 scanning electron microscope.

The Vickers hardness, HV, was measured at the cross section of the as-sprayed coating. The measured condition of Vickers hardness was: the loading weight was 0.196 N, the duration time was 15 s. The hardness of the coating was averaged by the 7 points measurement.

3. Results and discussion

3.1. X-Ray diffraction analysis

Fig. 1 shows the X-ray diffraction patterns of the powder and as-sprayed coating. It can be seen that there is no new phase in the coating and no clear difference of the peak intensities between the powder and coating. Both the powder and coating are composed of pure

tetragonal zirconia, which is the stable phase in the middle temperature. However, the X-ray pattern of the coating has two more peaks than that of the powder, it indicates that the coating has a better crystal structure than the powder. As we know, rapid solidification with a cooling rate of $\sim 10^6 \text{ K}\cdot\text{S}^{-1}$ can be achieved in the plasma spray process, and results in the fine crystallite structure of deposits. Evidently, the XRD peaks of the as-sprayed coating are narrowed in comparison to those of the starting powders, as a result of the grain growth. According to Eq. (1), the average grain size of the starting powder and as-sprayed coating were 23 and 89 nm, respectively. This indicates that although growth of nano powder grain took place, it was not very rapid during the plasma spraying process, and the coating remains nanostructured. In principle, the thermal history that the powders experience during thermal spraying can be mathematically described by a number of non-isothermal annealings. A theoretical framework that may be used to describe grain growth during non-isothermal annealing has been derived by Jiang et al.¹² From this work, the dependence of grain size on non-isothermal annealing can be theoretically predicted on the basis of Eq. (2).

$$D^n - D_0^n = \frac{AR}{v_0R} \left(T_f^2 \exp\left(-\frac{Q}{RT_f}\right) - T_i^2 \exp\left(-\frac{Q}{RT_i}\right) \right) \quad (2)$$

Where D is the mean grain size after an annealing time of t ; D_0 is the mean grain size at $t=0$; Q is the activation energy for isothermal grain growth and R the molar gas constant; T_i and T_f are the initial and final temperature (in absolute K), respectively.

As the heating rate increases, the increment of grain size decreases significantly, implying that a nanostructure may be retained at elevated temperature, if the heating rate is high enough, similar to that experienced by the injected powders during thermal spraying.

3.2. Microstructure of sprayed coating

The morphology of the starting powders was spherical or ellipsoidal with a size ranging from 10 to 40 nm in diameter, as shown in Fig. 2(a), and is in good agreement with that calculated by using the integral breadth method. Fig. 2(b) presents the surface microstructure of nanostructured zirconia coating, which shows that the coating is mainly composed of irregular-shaped fine grains with particles size ranging from 50 to 120 nm. Again, this is consistent with the result derived from Eq. (1). But nonetheless there were some larger particles of up to $\sim 1 \mu\text{m}$.

Fig. 3 presents the splat morphology of as-sprayed zirconia coating, which shows that it possesses two kinds of structure. One is the densely packed, overlapping

Table 1
Spraying parameters of nano ZrO_2 coating

Current	600A
Voltage	71V
Ar gas flow	40 slpm
H_2 gas flow	10 slpm
Carrier gas flow	3 slpm
Feeding distance(axial)	5 mm
Powder injector diameter	1.8 mm
Nozzle diameter	6 mm
Spray distance	100 mm
Torch traverse speed	9.7 mm/s
Substrate rotation speed	300 rpm

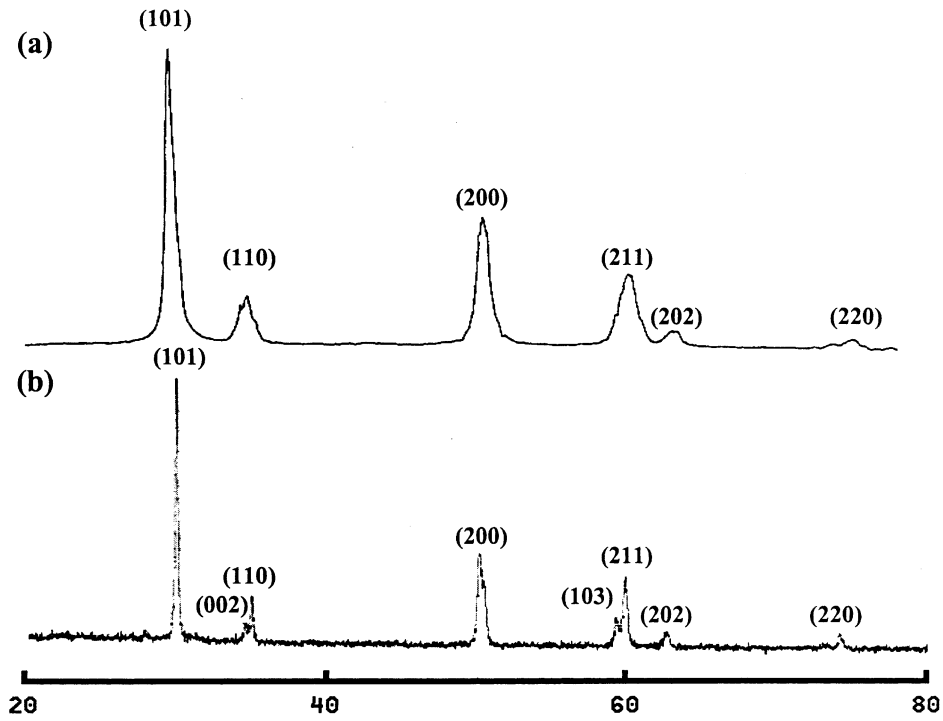


Fig. 1. XRD patterns of (a) starting ZrO₂ powder and (b) as-sprayed ZrO₂ coating layer.

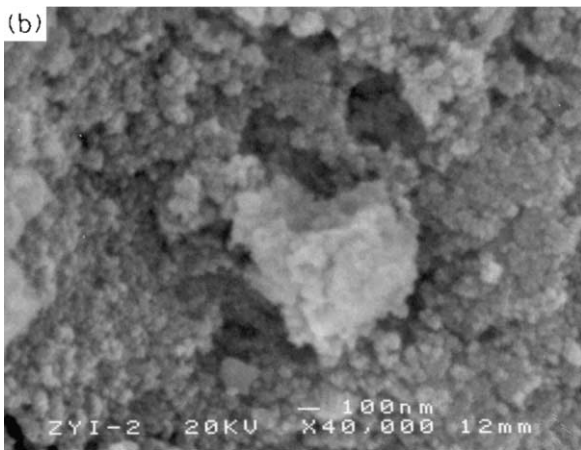
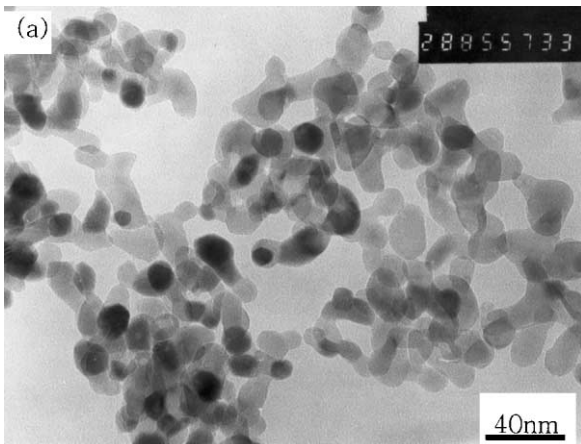


Fig. 2. The morphologies of (a) starting powder and (b) as-sprayed zirconia coating.

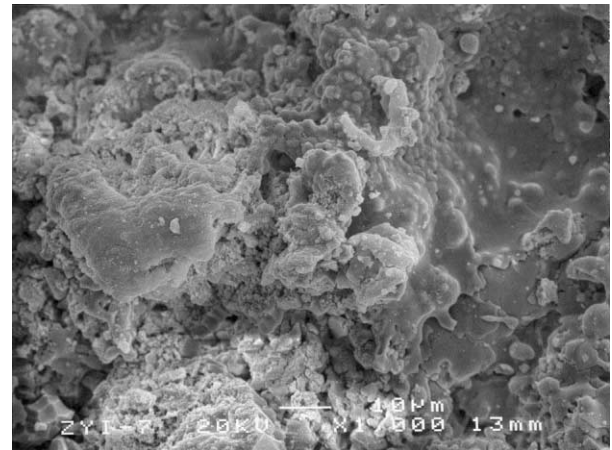


Fig. 3. Splat morphology of as-sprayed zirconia coating.

(pancake-like) splat, similar to a conventional thermal sprayed coating. The other appears to be poorly consolidated by fine particles, with no definite splat structure.

During the plasma spraying process, some nano starting powders are rapidly melted and according to Eq. (2), the growth of grain size is limited. This will result in the poorly consolidated structure because these droplets with fine grains also have low momentum on deposition. However, there exist some powders, which are heated at a lower rate in the plasma torch. Therefore, from Eq. (2), the grain size is expected to grow. These large grains impact the substrate with a higher momentum, and finally form the overlapping splat.

Fig. 4 shows the secondary electron image of the nano zirconia coating polished cross-section, which appears to be well bonded to the substrate. It should be noted that the thickness of coating is quite heterogeneous. The thickest section is up to 60 μm , while the thinnest region is only 10 μm . The thinner areas are also much denser than the thicker areas. Fig. 5 presents the cross-sectional

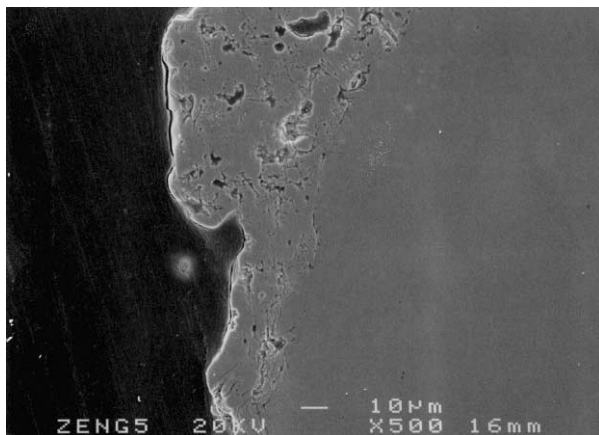


Fig. 4. SEM micrograph of cross-sectional area of nano zirconia coating.

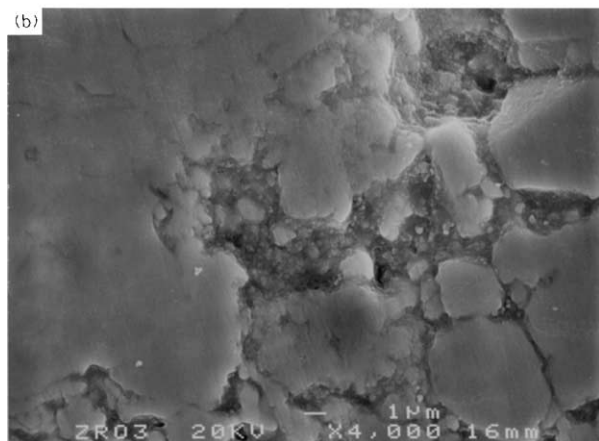
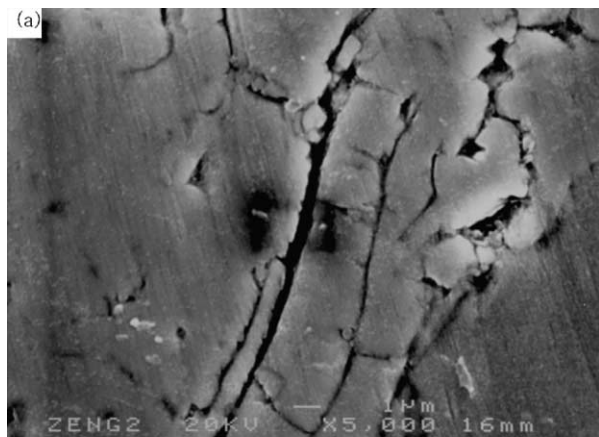


Fig. 5. The cross-sectional morphologies of (a) thin area and (b) thick area.

morphologies of thick and thin area. The thin area is the typical dense lamellar structure, which is revealed by the interlamellar microcracks. The thickness of each lamellar ranges from less than 1 to 3 μm , which is much thinner than that of conventional coating. As shown as Fig. 5(b), the thick area contains many unmelted particles, and the main reason that the thick area has much higher porosity than that in the thin area. A significant fraction of unmelted particles were wrapped into the melted droplet and impacted toward the substrate at high speed. This results in loose contact between the layers in the coating, increases the thickness, and forms the thicker areas.

3.3. Microhardness

The average Vickers hardness in the as-sprayed nano zirconia coating was $HV_{0.02} = 1320$, and is similar to that of ZrO_2 ceramic produced by the sintering. The noticeable increases in microhardness are observed in the nanocrystalline zirconia coating when compared with those of conventional counterpart. The Hall–Petch model, assuming on the basis that a dislocation network density within the nanoscale grains transfers slip through the grain boundaries, could explain it. However, the presence of pores in the coating will ultimately affect the microhardness measurements. Further studies by using nano indentation will give the more accurate results.

4. Conclusion

In this study, nanostructured zirconia coating is deposited by atmospheric plasma spraying. The ZrO_2 coating possesses two kinds of structure. One is the poorly consolidated structure, which is composed of nanosized particles. The other is overlapping structure, which is consisted of micrometer size particles. The former is the main structure in the coating. The zirconia coating has the same phase composition with the starting powder, which is pure tetragonal zirconia. The thickness of coating is quite heterogeneous. The unmelted particle is the main reason to result in the thicker coating. The as-sprayed nano zirconia coating has the similar microhardness with the sintering ZrO_2 ceramic, which is much higher than the conventional counterpart.

References

1. Yang, G., Zhuang, H. and Biswas, P., Characterization and nanophase titania particles processed in flame reactors. *Nanostructured Mater.*, 1996, 7(6), 676–689.
2. Hagfeldt, A., Valachopoulos, N. and Gratzel, M., Fast electrochromic switching with nanocrystalline oxide semiconductor films. *J. Electrochem. Soc.*, 1994, 47(7), 182–184.
3. Lu, J., Wang, J. and Rai, R., Solution precursor chemical vapor

- deposition of titanium oxide thin films. *Thin Solid Films*, 1991, **204**, 113–117.
4. Haro-Poniatowski, E., Rodriguez-Talavera, R., De La Cruz Hevedia, M., Cano-Corona, O. and Anoyo-Murillo, R., Crystallization of nanosized titania particles prepared by the sol-gel process. *J. Mater. Res.*, 1994, **9**, 2102–2108.
 5. Suhail, M. H., Rao, G. M. and Mohan, S., Dc reactive magnetron sputtering of titanium-structural and optical characterization of TiO₂ films. *J. Appl. Phys.*, 1992, **71**(3), 1421–1427.
 6. Li, H., Luo, W., Chen, X. and Zhuang, Z., Preparation of nanocrystalline PLT thin films by RF magnetron sputtering. *J. Inorg. Mater.*, 1994, **9**(3), 371–374.
 7. Karthikeyan, J., Berndt, C. C., Tikkanen, J., Wang, J. Y. and Herman, H., Preparation of nanophase materials by thermal spray processing of liquid precursor. *Nanostructured Mater.*, 1997, **9**, 137–140.
 8. Tellkamp, V. L., Lau, M. L., Fabel, A. and Lavernia, E. J., Thermal spraying of nanocrystalline Inconel 178. *Nanostructured Mater.*, 1997, **9**, 489–492.
 9. Berndt, C. C. and Lavernia, E. J., Thermal spray processing of nanoscale materials. *J. Thermal Spray Technol.*, 1998, **7**(3), 411–440.
 10. Zhu, Y., Huang, M., Huang, J. and Ding, C., Vacuum-plasma sprayed nanostructured titanium oxide films. *J. Thermal Spray Technology*, 1999, **8**(2), 219–222.
 11. Klug, H. P. and Alexander, L. E., *X-ray Diffraction Procedures*. John Wiley & Sons, New York, 1974, pp. 661–665.
 12. Jiang, H. G., Lau, M. L. and Lavernia, E. J., Thermal stability of nanocrystalline Inconel 718 and Ni prepared by high velocity oxy-fuel thermal spraying. In *Proceedings of the 15th International Thermal Spray Conference*, Nice, France, 1998, pp.1265–1269.